Progressive saturation NMR relaxation

V. F. Mitrović, E. E. Sigmund, and W. P. Halperin
Department of Physics and Astronomy, Northwestern University, Evanston, Illinois 60208
(Received 30 October 2000; revised manuscript received 9 February 2001; published 21 June 2001)

The NMR spin-lattice relaxation rate, T_1^{-1}, can be measured precisely by progressive saturation. This efficient technique is useful when T_1 is long and the NMR signal is weak. We derive the quasiequilibrium spin response to excitation in the case of a Zeeman spectrum in the presence of quadrupolar interactions. Exact solutions for the recovery of magnetization under the influence of purely magnetic fluctuations for $I=\frac{1}{2}$, $\frac{3}{2}$, and $\frac{5}{2}$ are presented. This is the general solution to a problem that has been previously solved only for the $I=\frac{1}{2}$ case. An important example for the application of this technique is ^{17}O NMR in cuprate superconductors ($I=\frac{5}{2}$). We show comparisons of the theory with the relaxation measured for high-temperature superconducting materials and the NMR-rates measured by this technique across the vortex-broadened spectrum at low temperature.

DOI: 10.1103/PhysRevB.64.024520 PACS number(s): 76.20.+q, 76.60.Es, 74.60.Ec

I. INTRODUCTION

There are frequent situations when NMR signals are weak and the relaxation times are so long that the spin-lattice relaxation experiment is arduous to perform with reasonable precision. For example, in high-temperature superconducting materials the NMR spin-lattice relaxation rate, T_1^{-1}, is small at low temperature owing to a decreasing number of normal quasiparticles. This is particularly true for ^{17}O and ^{89}Y nuclei. For the case of nuclei with $I=\frac{1}{2}$ it is well known that the most efficient way to determine the spin-lattice relaxation rate is by the method of progressive saturation.[1] However, the corresponding prescription for interpretation of progressive saturation experiments for quadrupolar nuclei under the influence of purely magnetic fluctuations has not been developed. In the case of purely quadrupolar relaxation, progressive saturation experiments were first performed and analyzed by Alexander and Tzalmona.[2] In our work we derive the quasistatic recovery profiles due to magnetic fluctuations for the quadrupolar-split Zeeman spectrum during progressive saturation making this technique a useful analytical tool. Then we compare the theory with experiment. The efficiency gained with our method over the standard relaxation measurement technique is of the order of the number of different delay times used in the experiment when more then three to four averages are used for the acquisition and can typically be as high as a factor of 30.

The heart of the progressive saturation method is that NMR spectra can be accumulated much faster and thus more accurately than the conventional measurement of the magnetization profile. In progressive saturation the repetition time, T_R, between consecutive spectrum acquisitions is varied and the effect on the amplitude of the signal is determined. In a conventional relaxation experiment each data acquisition consists of an excitation and detection of magnetization, and usually enough time is allowed between acquisitions, that the equilibrium spin temperature is fully restored, $T_R \geqslant 5T_1$. We refer to this in the following as the full-recovery method. In the case of progressive saturation thermal equilibrium is not established and the amplitude of the signal depends in general in a complicated way on the spin-lattice relaxation rate. The benefit in signal-to-noise from increasing the rate of data accumulation more than makes up for loss of signal from partial saturation. For spin $I=1/2$ the magnetization recovery profile for this progressive saturation experiment is easily obtained semiclassically. However, in order to measure T_1 of nuclei with $I>\frac{1}{2}$, with this method, it is necessary to derive magnetization recovery profiles as we present here. Then the spin-lattice relaxation rate can be obtained from a fit of the theoretical profile to the results of the progressive saturation experiment with a significant gain in efficiency.

The magnetization recovery for quadrupolar nuclei, after irradiation of a single transition, involves a sum of exponentials. Andrew and Tunstall[4] were the first to treat full-recovery relaxation in the case of quadrupolar-split Zeeman states for spin $I=\frac{3}{2},\frac{5}{2}$. The paper of Suter *et al.*[3] contains references to calculations of these multiexponential recovery profiles that are appropriate for what we call full-recovery experiments. In our work we derive the quasiequilibrium spin response to an excitation as a function of repetition time, T_R, and the NMR rate, T_1^{-1}, for a progressive saturation experiment. In these circumstances the populations of all the spin states deviate from their Boltzman distribution. We assume that the nuclei interact with an electric-field gradient (EFG), so that the Zeeman levels are unequally spaced to form $2I$ distinct satellite transitions, see Fig. 1. We consider the high-field limit so that Zeeman states are the system eigenstates, i.e., m is a good quantum number. We describe the progressive saturation experiment in Sec. II. In Sec. III we discuss basic principles and assumptions necessary to derive general recovery laws. Using this notation and these principles, we derive the progressive saturation recovery profiles in Sec. IV. We compare these profiles with the relaxation measured for high-temperature superconducting materials in Sec. V. Furthermore, we also show how this technique can be used to accurately measure the NMR rates across the broad spectra in these materials at low temperature.

II. PROGRESSIVE SATURATION EXPERIMENTS

In a progressive saturation experiment one does not wait for the magnetization to fully recover before repeating the

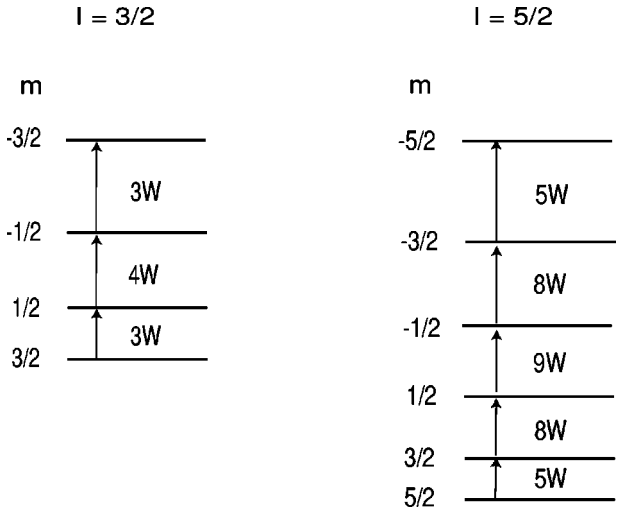

FIG. 1. Transitions between spin energy levels for $I=3/2$ and 5/2 caused by magnetic fluctuations. Only upward transitions are shown.

excitation and data-acquisition sequence. Consequently, the initial conditions for the spin system at the instant of excitation are not the Boltzmann thermal distribution for the level populations and the recovery profile as a function of T_R is quite different from that of the full-recovery method. The progressive saturation profiles have been worked out for a two-level system,[1,5] i.e., $I=1/2$. For higher spins, determination of the correct profile is a more complex task. A block diagram for a progressive saturation experiment is shown in Figs. 2 and 3 for one value of the repetition time T_R. We introduce a spin-manipulation operator $\tilde{\boldsymbol{\mathcal{S}}}$ that changes the level populations and also produces a detected signal such as an echo or free-induction decay. $\tilde{\boldsymbol{\mathcal{S}}}$ can be quite general including double resonance or multiple-pulse sequences. In many useful applications, such as we used to study high-temperature superconductors, the manipulation is a standard-Hahn echo, θ-τ-π-*acquire* sequence, which is repeated many times with a delay of T_R and then signal averaged in order to improve the signal-to-noise. The excitation strength is fixed by the tip angle θ. The process is repeated for a sufficient number of wait times $T_R \leqslant T_1$ to establish the recovery profile. We can assume that after the first-few pulses in each such sequence a quasiequilibrium in the spin system is established.[6] When we change T_R, we change the initial

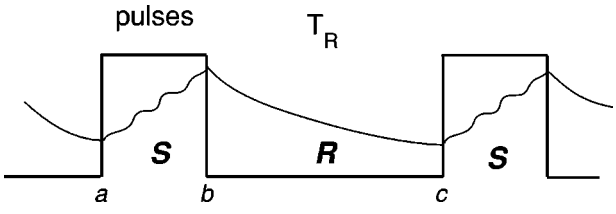

FIG. 2. Block diagram of our experiment. In the time interval between points *a* and *b* the spin evolution is described by the matrix $\tilde{\boldsymbol{\mathcal{S}}}$. During the time interval T_R the spins relax according to $\tilde{\boldsymbol{\mathcal{R}}}$. The deviation of the magnetization from its equilibrium value is sketched by curved lines.

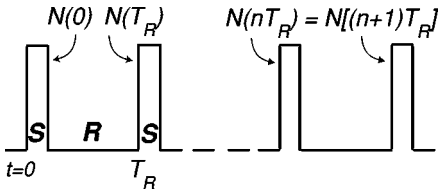

FIG. 3. Steady state, quasi-equilibrium, condition holds for sufficiently large *n*, when $\mathbf{N}(nT_R)=\mathbf{N}[(n+1)T_R]$.

conditions, at the instant of excitation, for the quasiequilibrium populations of the levels. With the progressive saturation experiment we can measure the magnetization as a function of T_R and extract the rate, T_1^{-1}. This is a much faster way of measuring the rate than the full-recovery experiment. For both methods the magnetization recovery profile is calculated theoretically and fit to the experimental measurement with three adjustable parameters: the equilibrium magnetization for the transition being excited, the excitation-pulse tip angle θ, and the spin-lattice relaxation rate.

III. MASTER EQUATION

The energy levels of a nucleus that possess spin I are split into $(2I+1)$ Zeeman energy levels in a magnetic field, H_0, each with energy $-m\gamma H_0\hbar$, proportional to its gyromagnetic ratio γ and spin quantum number m. Zeeman levels for nuclei with total spin $I=\frac{3}{2}$ and $\frac{5}{2}$ are schematically shown in Fig. 1. In addition to the static Zeeman interaction with H_0, we assume that there is a quadrupolar interaction between the nuclei and an EFG tensor. The quadrupolar interaction unequally shifts the Zeeman energy levels, sufficiently that they can be identified spectroscopically, but not so much that they significantly alter the levels, so that $2I$ distinct transitions are formed. This assumption is relevant only for the description of initial conditions and its implications will be discussed later in Sec. IV. We also assume the high-field limit where the Zeeman states are the system eigenstates, i.e., m is a good quantum number. Let a vector $\mathbf{p}_{0,m}$ represent the equilibrium population of the levels given by the Boltzmann distribution, $p_{0,m}\propto\exp(m\gamma H_0\hbar/k_BT)$. We also define vector $\mathbf{p}$ that represents the population of the levels, $\mathbf{P}$, minus the equilibrium population, $\mathbf{p}_0$, $\mathbf{p}=\mathbf{P}-\mathbf{p}_0$. The population difference between two adjacent levels is represented by a $2I$-dimensional vector $\mathbf{n}$. The equilibrium population difference between two adjacent levels $\mathbf{n}_0$ is given by,

$$\mathbf{n}_0=n_0\mathbf{1};\quad \mathbf{1}=\begin{pmatrix}1\\1\\\vdots\end{pmatrix},\quad n_0\propto\frac{\gamma H_0\hbar}{k_BT}. \tag{1}$$

We also define the population difference *minus the equilibrium population difference* between two adjacent levels as $\mathbf{N}$, $\mathbf{N}=\mathbf{n}-\mathbf{n}_0$.

The relaxation of the disturbed population $\mathbf{p}$ towards its equilibrium can be described by the master equation,[7]

$$\frac{d}{dt}\mathbf{p}=\tilde{\boldsymbol{\mathcal{W}}}\mathbf{p}, \tag{2}$$

where $\tilde{\mathcal{W}}$ is the $(2I+1)$-dimensional matrix whose elements, W_{mn}, are the transition probabilities from the state m to the state n, Fig. 1.

If the transitions are induced by magnetic fluctuations only $\Delta m = \pm 1$ transitions are allowed and the probabilities are given by,

$$W^{mag}_{m\to n=m\pm 1} = W(I\mp m)(I\pm m+1). \tag{3}$$

In the high-temperature limit, $\gamma H_0 \hbar \ll k_B T$, which is almost always satisfied in an NMR experiment, so that there is approximately equal probability for upward and downward transitions, i.e. $W^{mag}_{m\to m\pm 1} \approx W^{mag}_{m\pm 1\to m}$. Therefore, for magnetic fluctuations in the high-temperature limit, we can write the change of the population of the mth level as,

$$\frac{d\mathbf{p}_m}{dt} = W_{(m+1)\to m}\mathbf{p}_{m+1} - \{W_{m\to(m-1)} + W_{m\to(m+1)}\}\mathbf{p}_m + W_{(m-1)\to m}\mathbf{p}_{m-1}. \tag{4}$$

Since in an NMR experiment one detects a quantity proportional to the difference of population between two adjacent levels for the jth transition, one can rewrite the master Eq. (2), in terms of the population difference $\mathbf{N}$,

$$\frac{d}{dt}\mathbf{N} = \tilde{\mathcal{R}}\mathbf{N}, \tag{5}$$

where $\tilde{\mathcal{R}}$ now is a $2I$-dimensional matrix. The change of the population difference of the jth transition, between $m\to(m-1)$ levels, is given by,

$$\frac{d\mathbf{N}_j}{dt} = W_{(m+1)\to m}\mathbf{N}_{(j+1)} - \{2W_{m\to(m-1)}\}\mathbf{N}_j + W_{(m-1)\to m}\mathbf{N}_{(j-1)}. \tag{6}$$

The matrix $\tilde{\mathcal{R}}$ can then be obtained using Eq. (3) and Eq. (6). The full form of $\tilde{\mathcal{R}}$ for various spins is given in Appendix A. The eigenvalues and eigenvectors of $\tilde{\mathcal{R}}$ are λ_i and $\mathbf{E}_i$ respectively. The matrix $\tilde{E}$, composed of the eigenvectors $\mathbf{E}_i$, is defined so that $\tilde{E}^{-1}\tilde{\mathcal{R}}\tilde{E}$ is a diagonal matrix whose elements are the eigenvalues λ_i, i.e. $(\tilde{E}^{-1}\tilde{\mathcal{R}}\tilde{E})_{ij} = \lambda_i \delta_{ij}$. Equation (5) can then be rewritten as,

$$\frac{d}{dt}\mathbf{N} = \tilde{E}\lambda\tilde{E}^{-1}\mathbf{N}. \tag{7}$$

Defining a diagonal matrix $\tilde{\Lambda}$ as,

$$\tilde{\Lambda} = \begin{bmatrix} e^{\lambda_1 t} & 0 & 0 \\ 0 & \ddots & 0 \\ 0 & 0 & e^{\lambda_{2I} t} \end{bmatrix},$$

we can write the solution of Eq. (7),

$$\mathbf{N} = \tilde{E}\tilde{\Lambda}\tilde{E}^{-1}\mathbf{N}(0). \tag{8}$$

The vector $\mathbf{N}(0)$ describes the initial conditions of the spin system. Then Eq. (8) can be rewritten in the form,

$$N_j(t) = \sum_{i,k} (E_{ji}e^{\lambda_i t})E^{-1}_{ik}N_k(0). \tag{9}$$

In an NMR experiment, one measures the time-dependent z component of the magnetization for the jth transition, $\mathcal{M}_j(t)$, a quantity proportional to the difference of population between two adjacent levels. Thus once the elements of $\mathbf{N}(t)$ are known, the normalized magnetization recovery profile $\mathbf{M}(t)$ can be obtained as,

$$M_j(t) = \frac{\mathcal{M}_j(\infty) - \mathcal{M}_j(t)}{\mathcal{M}_j(\infty)} = -\frac{N_j(t)}{n_0}, \tag{10}$$

where $\mathcal{M}(\infty)$ is the equilibrium value of magnetization and the index j denotes the transition, i.e. the NMR line, that is observed. Substituting the expression for $N_j(t)$ from Eq. (9), $M_j(t)$ can be rewritten as

$$M_j(t) = -\sum_i c_i e^{\lambda_i t},$$

$$c_i = -\frac{1}{n_0}\sum_{j,k} E_{ij}E^{-1}_{jk}N_k(0). \tag{11}$$

This equation shows that after the initial preparation, described by $N_k(0)$, the magnetization recovery is a linear combination of exponentials of eigenvalues of the reduced recovery matrix.

IV. PROGRESSIVE SATURATION PROFILE

In this section we derive the quasiequilibrium spin response as a function of T_R and T_1. We will represent the disturbance of spin populations during excitation and detection by a matrix $\tilde{\mathcal{S}}$, $\mathbf{P}\to\mathbf{P}' = \tilde{\mathcal{S}}\mathbf{P}$. We assume that $T_2 \ll T_R$, so that all transverse coherence is lost during T_R. Knowledge of the detailed evolution of the magnetization-density matrix during pulsing is unnecessary. We consider the change in population of each Zeeman level. For the particular case of an irradiation of the jth transition the fractional population change (the depletion of the lower level and the enhancement of the upper-one normalized to their sum) can be described by a scalar, $\cos\theta$. In the semiclassical theory, θ is the tip angle. Thus, we define, for convenience a quantity $\mathcal{A} = -\frac{1}{2}(\cos\theta - 1)$ and write $\tilde{\mathcal{S}}$ as,

$$S_{jj} = -2\mathcal{A} + 1,$$

$$S_{jj\pm 1} = S_{j\pm 1 j} = \mathcal{A},$$

$$S_{j_1 j_2} = \delta_{j_1 j_2} \quad (j_1, j_2 \neq j),$$

$$\tilde{\mathcal{S}} \equiv \begin{bmatrix} 1 & & & & \\ & 1 & & & 0 \\ & & 1 & \mathcal{A} & \\ & & -2\mathcal{A}+1 & & \\ & 0 & & \mathcal{A} & \ddots \\ & & & & 1 \end{bmatrix}. \tag{12}$$

In the absence of an electric-field gradient, the Zeeman energy levels are equally spaced so that a pulse affects all transitions. In that case $\tilde{\mathcal{S}}$ has no zero elements.

After pulsing, the system starts to relax towards its equilibrium. This relaxation is described by the matrix $\tilde{\mathcal{R}}$. It is important to note that the system left to evolve under $\tilde{\mathcal{R}}$ can only evolve until the population difference reaches its equilibrium value, $\mathbf{n}_0$. One can say that $\tilde{\mathcal{R}}$ acts only on **N** space, affecting only the population difference in excess of $\mathbf{n}_0$. On the other hand, $\tilde{\mathcal{S}}$ acts on **n** space, altering absolute population differences.

After n-acquired spectra the condition for quasiequilibrium is that $\mathbf{N}(nT_R)$ is equal to $\mathbf{N}[(n+1)T_R]$ as shown in Fig. 3. Thus we can write,

$$\mathbf{N}[(n+1)T_R] = \mathbf{N}(nT_R). \tag{13}$$

Since $\tilde{\mathcal{S}}$ acts on **n** space and $\tilde{\mathcal{R}}$ on **N**, the steady-state condition, Eq. (13), can be written as,

$$\begin{aligned} \mathbf{N}[(n+1)T_R] &= \tilde{E}\tilde{\Lambda}\tilde{E}^{-1}[\tilde{\mathcal{S}}\{\mathbf{N}(nT_R)+\mathbf{n}_0\}-\mathbf{n}_0], \\ &= \mathbf{N}(nT_R). \end{aligned} \tag{14}$$

A. $I=1/2$

Here we show that Eq. (14) has a simple solution for a two-level system enabling us to make a direct comparison with its semiclassical solution. For $I=1/2$, $\tilde{\mathcal{S}}=\cos\theta$, and $\tilde{E}\tilde{\Lambda}\tilde{E}^{-1}=e^{-2WT_R}=e^{-T_R/T_1}$. Substituting in Eq. (14) we obtain,

$$N = e^{-T_R/T_1}[\cos\theta(N+n_0)-n_0]. \tag{15}$$

Solving for N we find,

$$\frac{N}{n_0} = \frac{e^{-T_R/T_1}(\cos\theta-1)}{(1-e^{-T_R/T_1}\cos\theta)}, \tag{16}$$

an expression identical to the one obtained from the semiclassical treatment of the problem.[1] Note that Eq. (16) has the correct limits $\lim_{T_R\to\infty}(N/n_0)=0$ and $\lim_{T_R\to 0}(N/n_0)=-1$.

B. General I

For a general spin, I, Eq. (14) can be solved in the following way,

$$\mathbf{N}[(n+1)T_R] = \mathbf{N}(nT_R) = \mathbf{N} = \tilde{E}\tilde{\Lambda}\tilde{E}^{-1}(\tilde{\mathcal{S}}\mathbf{N}+\tilde{\mathcal{S}}\mathbf{n}_0-\mathbf{n}_0). \tag{17}$$

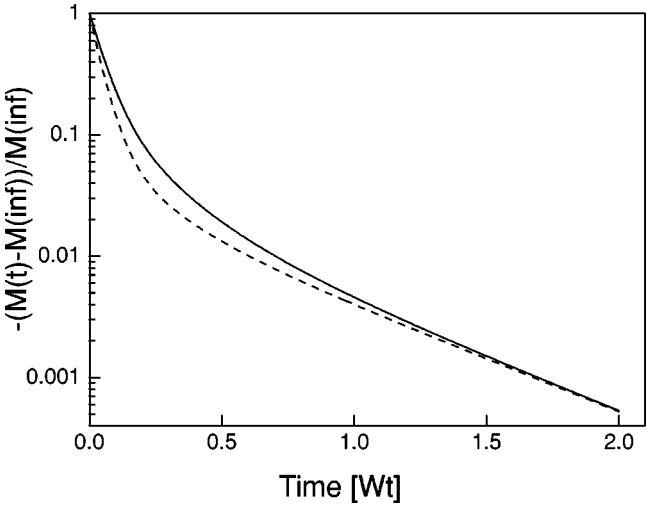

FIG. 4. Comparison of recovery profiles for progressive saturation (solid line) and full-recovery (dashed line) experiment ($\pm\frac{3}{2}\leftrightarrow\pm\frac{1}{2}$) transition for $I=5/2$, $\pi/2$ tip angle. The full-recovery profile $\propto$ ($\frac{2}{35}e^{-2Wt}+\frac{3}{28}e^{-6Wt}+\frac{1}{20}e^{-12Wt}+\frac{25}{28}e^{-20Wt}+\frac{25}{28}e^{-30Wt}$).

Knowing that $\tilde{\mathcal{S}}$ is linear, we can easily solve Eq. (17) for **N**,

$$\mathbf{N} = (\tilde{1}-\tilde{E}\tilde{\Lambda}\tilde{E}^{-1}\tilde{\mathcal{S}})^{-1}\tilde{E}\tilde{\Lambda}\tilde{E}^{-1}(\tilde{\mathcal{S}}-\tilde{1})\mathbf{n}_0. \tag{18}$$

From Eq. (18) the general matrix equation for recovery profiles for all transitions for an arbitrary spin system I can be obtained,

$$\mathbf{M}(t) = -(\tilde{1}-\tilde{E}\tilde{\Lambda}\tilde{E}^{-1}\tilde{\mathcal{S}})^{-1}\tilde{E}\tilde{\Lambda}\tilde{E}^{-1}(\tilde{\mathcal{S}}-\tilde{1})\mathbf{1}. \tag{19}$$

This relation is general to many types of NMR experiments such as double resonance or multiple pulse sequences. For the particular case of the Hahn-echo irradiation of the jth level the form of $\tilde{S}$ is given by Eq. (12).

V. DISCUSSIONS AND COMPARISON WITH EXPERIMENT

In Appendix B, we give recovery profiles for $I=\frac{3}{2}$ and $I=\frac{5}{2}$ obtained from Eq. (19). Comparison between the recovery profiles for the progressive saturation and excitation full-recovery experiment is shown in Fig. 4.

We have compared the values of T_1 extracted from a full-recovery experiment, $\pi/2-\tau_1-\pi/2-\tau-\pi$, and progressive saturation experiment for the $-\frac{3}{2}\leftrightarrow-\frac{1}{2}$ transition of an $I=\frac{5}{2}$ system, planar ^{17}O in YBCO, at 100 K. The recovery data for these two experiments and their corresponding fits are shown in Fig. 5. Fitting each to the appropriate profile for T_1 and tip angle the same values were obtained within the error bars of $\pm 3\%$. In general, in order to determine T_1 within a precision of a few percent the progressive saturation experiment requires typically 30 times less time to run than the full recovery when substantial averaging is needed.

Due to the complexity of the progressive saturation profiles a nonlinear least-squares fit must be performed to extract the three parameters T_1, $\mathcal{M}(\infty)$, and the tip angle θ. However errors in T_1 and θ are correlated such that a sys-

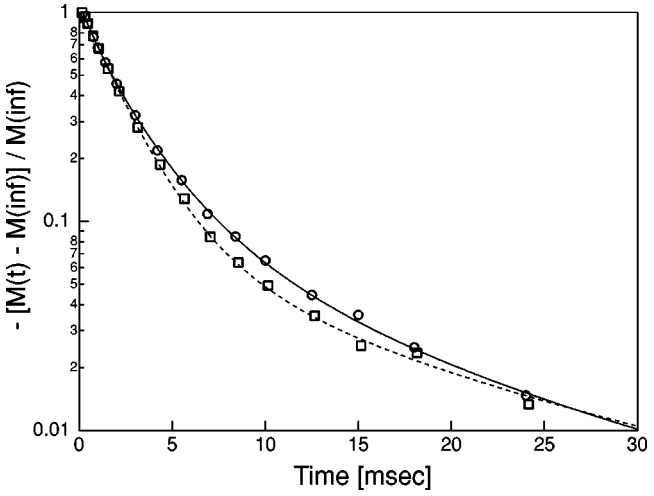

FIG. 5. Comparison of recovery data for progressive saturation (open circles) and full-recovery (open squares) experiment for $(\pm\frac{3}{2}\leftrightarrow\pm\frac{1}{2})$ transition of ^{17}O ($I=\frac{5}{2}$) in YBCO at 100 K. Fits are shown for the corresponding recovery profiles, progressive saturation (solid line), $\theta=64°$, $T_1=27.03$ ms, and full recovery (dashed line), $\theta=75°$, $T_1=25.64$ ms. Note that the recovery-curves cross at ~ 27 ms due to different θ.

tematic error of $\pm 1\%$ in the tip angle produces a corresponding error of $\sim\pm 5\%$ in T_1. Typically the statistical error in determining the tip angle is $\sim\pm 0.5\%$. Nonuniformity of the rf excitation, i.e., the H_1 field, can also lead to systematic error in T_1. Such inaccuracy can be independently determined through direct comparison of at least one measurement of T_1 by progressive saturation with a measurement by full recovery under the same controlled conditions. In many instances precision of the measurement is required in order to explore variations with magnetic field or temperature. Then the tip angle is fixed at an optimal value that minimizes χ^2 and the variations of T_1 can be determined with a precision of better than $\pm 1\%$.

The ratio of the total time needed for a full-recovery (FR) experiment relative to a progressive saturation (PS) experiment for the same signal-to-noise in extracting T_1 is approximately,

$$R_{tot}\approx\frac{N_{swFR}}{N_{swPS}}*\frac{3}{2}N_d. \tag{20}$$

Here, N_d is the number of different delay times between excitation and detection in the full-recovery experiment or the number of different T_R in the progressive saturation experiment and is typically 20 to 30; N_{swFR} and N_{swPS} are the numbers of total averages per delay time. Only several (~ 4) pulses are required to establish the quasiequilibrium condition (see Fig. 3). We have compared the progressive saturation profiles and extracted rates when the number of initial excitations (prior to acquisition) was varied from 4 to 16. The values of the extracted rates varied within the error bars. The progressive saturation method is not that favorable if T_1 can be measured in a single acquisition. In this $R_{tot}\propto(3/8)N_d$. On the other hand, if we need to perform more than 100 averages the progressive saturation experiment requires less running time by a factor of $\sim\frac{3}{2}N_d$. Similarly, if T_1 is shorter than the minimum spectrometer acquisition reset time, the progressive saturation method does not offer a major savings in the running time. The method becomes more favorable as T_1 increases and as the required number of averages increases.

In order to measure T_1 within the error bars of $\pm 3\%$ the longest T_R in the progressive saturation experiment should be between 0.5–0.7 of T_1, so that the curvature in the recovery profiles shown in Fig. 5 can be covered. The curvature in the recovery profiles also depends on the tip angle. It is impossible to know the exact tip angle *a priori* and this is particularly true in the case of broader lines, often encountered in solids. Thus, it is important to take data for T_R as long as 0.5–0.7 T_1 in order to measure T_1 to a precision of several percent.

Very often, in solid state NMR, broad lines are encountered that extend beyond the bandwidth of a typical NMR pulse. In this situation one can use a field-sweep technique to determine the accurate line shape.[10,11] Combined with the progressive saturation technique, field sweep enables one to measure precisely variations in the NMR rate across a broad spectrum (provided there is no major spin-diffusion contribution to the rate). In this experiment the external magnetic field is changed while the probe is tuned and spectrometer set to a fixed frequency. At each value of the field, a progressive saturation experiment is carried out. Spectra, after signal averaging, at each value of the field are added together to obtain total composite spectra for a particular value of T_R. The progressive saturation and field-sweep experiments complement each other giving us a powerful technique for measuring long T_1 for broad spectra. It enables faster-experimental execution, leading to high signal-to-noise, while still assuring that the entire spectrum is covered. Furthermore, the spectrometer gain and sensitivity stay constant throughout the experiment so that the rates at every point in the spectrum are measured under the same conditions.

It is particularly useful to use this combined technique to measure T_1 in high-temperature superconducting materials at low temperatures where the rates become very slow due to the decreasing number of normal quasiparticles. Study of the low-temperature rate enables one to probe the dynamics of low-energy quasiparticle excitations, which dictate the thermodynamic properties of the material. If one is to measure these rates precisely, the problems of broad lines and slow rates have to be circumvented. Both ^{63,65}Cu and ^{17}O lines broaden at low temperatures and high-magnetic field owing to appearance of stationary vortices.[8,9] The broadening is beyond the bandwidth of a typical NMR pulse. Thus, one cannot use the Fourier transform of a Hahn echo to accurately measure the entire line shape. We have used the progressive saturation technique combined with field sweep, as described here, to determine both the accurate line shape of ^{17}O in the vortex-lattice state and the rates across that spectrum as shown in Fig. 6. The NMR rate increases by ~ 4 on moving to the right in Fig. 6, i.e., approaching the vortex core. This increase in the rate is expected from nuclear spin-flip scattering by Doppler-shifted *d*-wave quasiparticles.[12–14]

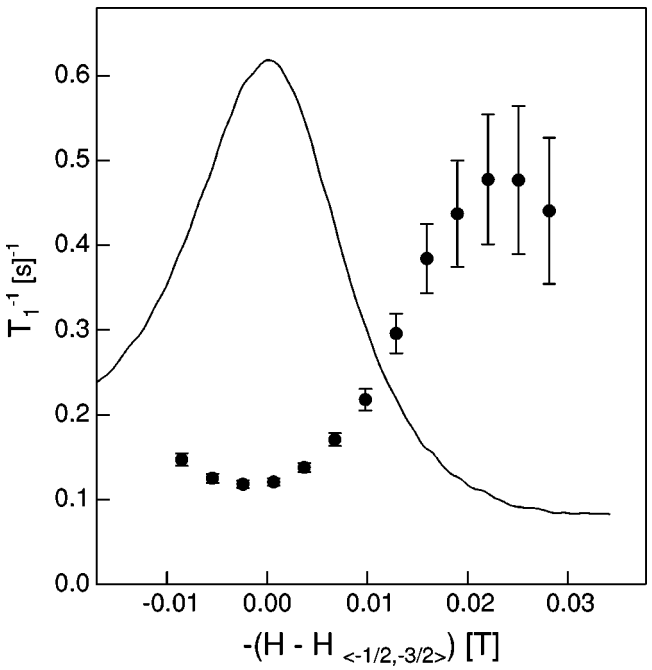

FIG. 6. Planar ^{17}O spin-lattice relaxation rate (data points), extracted from a corresponding portion of the spectrum (smooth curve), inhomogeneously broadened by the vortex lattice in $YB_2C_3O_{7-\delta}$ at 11 K and 13 T. The spectrum represents the $(\pm\frac{3}{2}\leftrightarrow\pm\frac{1}{2})$ transition. The tip angle was established to be $\theta=65.5°$.

VI. CONCLUSIONS

We have calculated progressive saturation magnetization recovery profiles for general spin I, for the spin system whose Zeeman states are unequally split by quadrupolar interactions. We have assumed that the relaxation of the magnetization is magnetic in origin so that $m\leftrightarrow m\pm1$ are the only allowed transitions. We argue that the progressive saturation experiment is a powerful technique for measuring long T_1 as is the case, for example, in high-temperature superconducting materials at low temperatures. It enables one to do the experiment much faster and obtain better signal-to-noise ratio.

ACKNOWLEDGMENT

We are grateful to M. Eschrig for useful discussions. This work was supported by the National Science Foundation, Grant No. DMR 91-20000, through the Science and Technology Center for Superconductivity.

APPENDIX A: $\tilde{\mathcal{R}}$, REDUCED RECOVERY MATRICES

$\tilde{\mathcal{R}}$ matrix for $I=\frac{1}{2}$

$$\tilde{\mathcal{R}}_{\frac{1}{2}}=-2W. \tag{A1}$$

$\tilde{\mathcal{R}}$ matrix for $I=\frac{3}{2}$

$$\tilde{\mathcal{R}}_{\frac{3}{2}}=W\begin{bmatrix}-6&4&0\\3&-8&3\\0&4&-6\end{bmatrix}. \tag{A2}$$

$\tilde{\mathcal{R}}$ matrix for $I=\frac{5}{2}$

$$\tilde{\mathcal{R}}_{\frac{5}{2}}=W\begin{bmatrix}-10&8&0&0&0\\5&-16&9&0&0\\0&8&-18&8&0\\0&0&9&-16&5\\0&0&0&8&-10\end{bmatrix}. \tag{A3}$$

Note that $(1/T_1)\equiv 2W$.

APPENDIX B: RECOVERY PROFILES FOR $I=\frac{3}{2}$ AND $\frac{5}{2}$

The following magnetization recovery profiles are obtained by using Eq. (19) and taking into account only the transitions, $m\leftrightarrow m\pm1$, induced by fluctuating magnetic fields. We have assumed that the Zeeman levels are unequally spaced, by the quadrupolar interaction, so that the matrix $\tilde{\mathcal{S}}$ is defined as in Eq. (12). In the absence of the quadrupolar interaction, $\tilde{\mathcal{S}}$ has no zero elements, since a pulse affects all the transitions simultaneously, and more complicated recovery profiles, not included in this paper, are obtained.

Recovery profiles for spin $I=3/2$

$$\frac{N}{n_0}\left(-\frac{1}{2}\leftrightarrow\frac{1}{2}\right)=\frac{-\mathcal{A}e^{-2Wt}(10e^{-10Wt}+e^{-8Wt}+e^{-6Wt}+e^{-4Wt}+e^{-2Wt}+1)}{5(1-e^{-12Wt})+\mathcal{A}\cdot(10e^{-12Wt}+e^{-10Wt}+e^{-8Wt}+e^{-6Wt}+e^{-4Wt}+e^{-2Wt})}. \tag{B1}$$

$$\frac{N}{n_0}\left(\pm\frac{3}{2}\leftrightarrow\pm\frac{1}{2}\right)=\frac{-\mathcal{A}e^{-2Wt}(10e^{-10Wt}+e^{-8Wt}+e^{-6Wt}+6e^{-4Wt}+e^{-2Wt}+1)}{5(1-e^{-12Wt})+\mathcal{A}(10e^{-12Wt}+e^{-10Wt}+e^{-8Wt}+6e^{-6Wt}+e^{-4Wt}+e^{-2Wt})}. \tag{B2}$$

Recovery profiles for spin $I=5/2$

$$\begin{aligned}\frac{N}{n_0}\left(-\frac{1}{2}\leftrightarrow\frac{1}{2}\right)=&-2\mathcal{A}e^{-2Wt}(315e^{-34Wt}+9e^{-32Wt}+9e^{-30Wt}+324e^{-28Wt}+18e^{-26Wt}+18e^{-24Wt}+74e^{-22Wt}\\&+18e^{-20Wt}+18e^{-18Wt}+74e^{-16Wt}+18e^{-14Wt}+18e^{-12Wt}+74e^{-10Wt}+18e^{-8Wt}+18e^{-6Wt}+9e^{-4Wt}\\&+9e^{-2Wt}+9)/[315(1+e^{-6Wt}-e^{-36Wt}-e^{-30Wt})+\mathcal{A}(630e^{-36Wt}+18e^{-34Wt}+18e^{-32Wt}+648e^{-30Wt}\end{aligned}$$

$$+36e^{-28Wt}+36e^{-26Wt}+148e^{-24Wt}+36e^{-22Wt}+36e^{-20Wt}+148e^{-18Wt}+36e^{-16Wt}+36e^{-14Wt}$$
$$+148e^{-12Wt}+36e^{-10Wt}+36e^{-8Wt}+18e^{-6Wt}+18e^{-4Wt}+18e^{-2Wt}). \quad \text{(B3)}$$

$$\frac{N}{n_0}\left(\pm\frac{3}{2}\leftrightarrow\pm\frac{1}{2}\right)=-\mathcal{A}e^{-2Wt}(280e^{-42Wt}-272e^{-40Wt}+280e^{-38Wt}+23e^{-36Wt}-7e^{-34Wt}+303e^{-32Wt}-242e^{-30Wt}+266e^{-28Wt}$$
$$+53e^{-26Wt}+16e^{-24Wt}+141e^{-22Wt}-72e^{-20Wt}+141e^{-18Wt}+16e^{-16Wt}+53e^{-14Wt}-14e^{-12Wt}+38e^{-10Wt}$$
$$+23e^{-8Wt}-7e^{-6Wt}+23e^{-4Wt}+8)/[140(1-e^{-2Wt}+e^{-4Wt}+e^{-10Wt}-e^{-12Wt}+e^{-14Wt}-e^{-30Wt}+e^{-32Wt}$$
$$-e^{-34Wt}-e^{-40Wt}+e^{-42Wt}-e^{-44Wt})+\mathcal{A}(280e^{-44Wt}-272e^{-42Wt}+280e^{-40Wt}+23e^{-38Wt}-7e^{-36Wt}$$
$$+303e^{-34Wt}-242e^{-32Wt}+266e^{-30Wt}+53e^{-28Wt}+16e^{-26Wt}+141e^{-24Wt}-72e^{-22Wt}+141e^{-20Wt}$$
$$+16e^{-18Wt}+53e^{-16Wt}-14e^{-14Wt}+38e^{-12Wt}+23e^{-10Wt}-7e^{-8Wt}+23e^{-6Wt}+8e^{-2Wt})]. \quad \text{(B4)}$$

$$\frac{N}{n_0}\left(\pm\frac{5}{2}\leftrightarrow\pm\frac{3}{2}\right)=-\mathcal{A}e^{-2Wt}(70e^{-42Wt}-68e^{-40Wt}+70e^{-38Wt}+17e^{-36Wt}-13e^{-34Wt}+87e^{-32Wt}-23e^{-30Wt}+29e^{-28Wt}$$
$$+62e^{-26Wt}+4e^{-24Wt}+24e^{-22Wt}+42e^{-20Wt}+24e^{-18Wt}+4e^{-16Wt}+62e^{-14Wt}-41e^{-12Wt}+47e^{-10Wt}$$
$$+17e^{-8Wt}-13e^{-6Wt}+17e^{-4Wt}+2)/[35(1-e^{-2Wt}+e^{-4Wt}+e^{-10Wt}-e^{-12Wt}+e^{-14Wt}-e^{-30Wt}+e^{-32Wt}$$
$$-e^{-34Wt}-e^{-40Wt}+e^{-42Wt}-e^{-44Wt})+\mathcal{A}(70e^{-44Wt}-68e^{-42Wt}+70e^{-40Wt}+17e^{-38Wt}-13e^{-36Wt}$$
$$+87e^{-34Wt}-23e^{-32Wt}+29e^{-30Wt}+62e^{-28Wt}+4e^{-26Wt}+24e^{-24Wt}+42e^{-22Wt}+24e^{-20Wt}+4e^{-18Wt}$$
$$+62e^{-16Wt}-41e^{-14Wt}+47e^{-12Wt}+17e^{-10Wt}-13e^{-8Wt}+17e^{-6Wt}+2e^{-2Wt})]. \quad \text{(B5)}$$

All of the above recovery profiles have the right limits, $\lim_{T_R\to\infty}(N/n_0)=0$ and $\lim_{T_R\to 0}(N/n_0)=-1$.

[1] E. Fukushima and S. B. W. Roeder, *Experimental Pulse NMR, A Nuts and Bolts Approach* (Addison-Wesley, Reading, MA, 1981).
[2] S. Alexander and A. Tzalmona, Phys. Rev. **138**, A845 (1965).
[3] A. Suter, M. Mali, J. Roos, and D. Brinkmann, J. Phys.: Condens. Matter **10**, 5977 (1998).
[4] E. Andrew and D. Tunstall, Proc. Phys. Soc. Jpn. **78**, 1 (1961).
[5] B. Cowan, *Nuclear Magnetic Resonance and Relaxation* (Cambridge University Press, U.K., 1997).
[6] R. Freeman and H. D. W. Hill, J. Chem. Phys. **54**, 3367 (1971).
[7] A. Abragam, *Principles of Nuclear Magnetism* (Oxford University Press, Oxford, 1961).
[8] A. P. Reyes, X. P. Tang, H. N. Bachman, W. P. Halperin, J. A. Martindale, and P. C. Hammel, Phys. Rev. B **55**, R14 737 (1997).
[9] M. Takigawa, P. C. Hammel, R. H. Heffner, Z. Fisk, J. D. Thompson, and M. Maley, Physica C **162-164**, 175 (1989).
[10] W. G. Clark, M. E. Hanson, F. Lefloch, and P. Ségransan, Rev. Sci. Instrum. **66**, 2453 (1995).
[11] V. F. Mitrović, E. E. Sigmund, H. N. Bachman, W. P. Halperin, A. P. Reyes, P. Kuhns, and W. G. Moulton (unpublished).
[12] M. Takigawa, M. Ichioka, and K. Machida, Phys. Rev. Lett. **83**, 3057 (1999).
[13] R. Wortis, A. J. Berlinsky, and C. Kallin, Phys. Rev. B **61**, 12 342 (2000).
[14] D. K. Morr and R. Wortis, Phys. Rev. B **61**, R882 (2000).